Geofluids (2007) 7, 258–269 doi:10.1111/j.1468-8123.2007.00179.x

Solubility of corundum + kyanite in H_2O at 700°C and 10 kbar: evidence for Al-Si complexing at high pressure and temperature

C. E. MANNING

Department of Earth and Space Sciences, University of California, Los Angeles, CA, USA

ABSTRACT

The solubility of the assemblage corundum + kyanite in H_2O was determined at 700°C and 10 kbar, using a piston-cylinder apparatus and rapid-quench/fluid-extraction techniques. Weighted mean concentrations of total Al and Si were 5.80 ± 0.03 mmol kg^{-1} H_2O and 0.308 ± 0.003 mol kg^{-1} H_2O, respectively (1σ errors). The Al concentration is nearly five times higher than that of corundum solubility in pure H_2O. This difference is interpreted to arise from complexing between Si and Al to form $HAlSiO_{4,aq}$ species. Charged or more polymerized species are also possible, but their abundance cannot be constrained based on these experiments. Assumption of a single aqueous aluminosilicate complex permits calculation of the thermodynamic consequences of Al-Si interaction in high-pressure fluids, as well as phase diagrams for the system Al-Si-O-H. Formation of Al-Si complexes leads to a large increase in dissolved Al with increasing Si in solution, such that Al concentration in equilibrium with kyanite + quartz is predicted to be 7.1 mmolal, higher than with kyanite + corundum. The elevated concentration of Si in deep-crustal and mantle aqueous fluids suggests that Al must readily be dissolved and transported by Al-Si complexing in high-pressure metamorphic and metasomatic environments. The results provide a simple explanation for the common observation of kyanite + quartz segregations in eclogites and Barrovian metamorphic rocks.

Key words: aluminium mobility, corundum solubility, crustal fluids, hydrothermal experiments.

Received 1 November 2006; accepted 20 January 2007

Corresponding author: C. E. Manning, Department of Earth and Space Sciences, University of California, Los Angeles, CA 90095-1567, USA.
Email: manning@ess.ucla.edu. Tel: 310 206 3290. Fax: 310 825 2779.

Geofluids (2007) 7, 258–269

INTRODUCTION

Studies of compositional change during metamorphism require an appropriate geochemical reference frame, in which an extensive parameter such as volume, mass, or element concentration is conserved (e.g., Irving 1911; Lindgren 1912, 1918; Ridge 1949; Poldervaart 1953; Gresens 1967; Grant 1986). In a classic study, Carmichael (1969) concluded that a constant-Al reference frame was supported by the small scale and magnitude of Al mobility during amphibolite-grade metamorphism of pelites in several localities. The inference was based on metamorphic reaction textures, and supported by low inferred solubility and diffusivity of Al in metamorphic fluids. Carmichael (1969) used these observations to explain textures of prograde mineral growth. Although he noted that a constant-Al reference frame was unlikely to pertain to all cases, Carmichael's approach has been applied in many subsequent studies, leading to widespread assumption that, to first order, Al is immobile in metamorphism and metasomatism.

In contrast, some studies of metamorphic textures have suggested that Al may be mobile in geologic fluids (e.g., Yardley 1977; Vernon 1979). Significant Al mobility during metamorphism is supported by occurrences of Al-rich minerals such as aluminosilicates (Al_2SiO_5) in veins and segregations, which imply at least local metasomatic transfer of Al (Kerrick 1988, 1990; Cesare 1994; Ague 1995; Nabelek 1997; Whitney & Dilek 2000; Widmer & Thompson 2001; McLelland *et al.* 2002; Sepahi *et al.* 2004). In the absence of evidence for unusually high fluid fluxes, such observations require high Al solubility and/or mobility in metamorphic

fluids. Thus, Al may be locally conserved during some metamorphic and metasomatic processes, but there are many other cases in which it appears to be quite mobile.

Element mobility requires elevated diffusivity and/or solubility. If the diffusion coefficient for Al is low compared to other species, it will be less readily transported in a given chemical potential gradient. Aqueous diffusion coefficients at fixed pressure (*P*) and temperature (*T*) decrease with increasing charge, though the effect is modest at high *P* and *T* (Oelkers & Helgeson 1988). Thus, Al^{+3} diffusivity is expected to be lower than monovalent or divalent cations, as inferred by Carmichael (1969). However, Al^{+3} will only be present at extremely low pH at most metamorphic *P* and *T*. Instead, the predominant Al hydroxide species over a wide range of pH are $Al(OH)_3^{\circ}$ and $Al(OH)_4^-$ (Pokrovskii & Helgeson 1995), for which diffusion coefficients should be similar to other neutral and monovalent species. Significantly lower diffusivity of Al than for other elements in metamorphic fluids is therefore unlikely, as has been shown experimentally by Vidal & Durin (1999) and Verlaguet *et al.* (2006).

A second control on mobility is the capability of metamorphic fluids to dissolve Al. Experiments on corundum solubility in H_2O at low pressure (<3 kbar) and a wide range of metamorphic temperatures indicate low Al concentrations (e.g., Morey 1957; Anderson & Burnham 1967; Burnham *et al.* 1973; Becker *et al.* 1983; Ragnarsdóttir & Walther 1985; Walther 1997). Corundum solubility in pure H_2O increases with pressure (Becker *et al.* 1983; Tropper & Manning 2007), but the effect is small: for example, at 700°C, Al concentration in H_2O in equilibrium with corundum rises from 0.04 mmolal at 2 kbar to 1.2 mmolal at 10 kbar (Tropper & Manning 2007), indicating that although there is a large relative increase, the total corundum solubility in H_2O at high *P* is still quite low. However, crustal and mantle fluids contain other dissolved constituents with which Al might interact. Mechanisms proposed for increasing Al solubility include H^+ metasomatism by acidic solutions (Gresens 1971; Vernon 1979; Ague 1994; Zaraisky 1994; Nabelek 1997; McLelland *et al.* 2002) and complexing with alkalis and/or halides (Anderson & Burnham 1967, 1983; Korzhinskiy 1987; Sanjuan & Michard 1987; Pascal & Anderson 1989; Pokrovskii & Helgeson 1995, 1997; Azaroual *et al.* 1996; Diakonov *et al.* 1996; Tagirov & Schott 2001; Walther 2001; Newton & Manning 2006). A potential complexing agent that has received only minor attention is Si. Al-Si complexing has been inferred at low *P* and *T* in acidic and basic solutions (Pokrovski *et al.* 1996; Salvi *et al.* 1998). Given that Si is quite concentrated in high-*P* fluids, it is possible that Al solubility could be strongly influenced by Al-Si interaction in the aqueous phase. However, no experimental studies have addressed this problem at deep-crustal and upper-mantle conditions.

This article presents new data on Al in metamorphic fluids based on experiments that constrain equilibrium solubility of the assemblage corundum + kyanite in Si-bearing H_2O at 10 kbar and 700°C. The results demonstrate that Al is substantially more soluble in Si-rich solutions than in pure H_2O at the same conditions. The data permit derivation of thermodynamic properties of a hypothetical Al-Si species, and show that aqueous Al will predominantly occur as Al-Si complexes over a wide range of silica activities.

METHODS

For each experiment, several 4–5 mm cleavage flakes were taken from gem-quality kyanite crystals from Bahia, Brazil (0.20 wt.% Fe_2O_3; Bohlen *et al.* 1991) and loaded into Pt capsules (5 mm O.D.) with 50–75 μl of nanopure H_2O. In several cases, finely ground Brazilian quartz (Manning 1994), reagent grade γ-Al_2O_3, and/or a corundum chip from a pure, flux-grown single crystal (Newton & Manning 2006) were also added. The quartz and γ-Al_2O_3 were ground for approximately 30 min in a mortar and pestle prior to loading. Kyanite grains were contained within crimped inner Au capsules (2 mm O.D.). This arrangement helped prevent crystal breakage while allowing the solution to react with the kyanite. Outer Pt capsules were sealed by arc welding. Reported H_2O mass reflects the weight prior to welding. Weight is lost on capsule sealing owing to minor vaporization of Pt and H_2O, but weight losses during welding were usually small (typically 0.1 mg).

Experiments were conducted in an end-loaded piston-cylinder apparatus with 2.54 cm diameter NaCl-graphite-BN furnace assemblies (Manning & Boettcher 1994). Temperature was controlled using Pt-$Pt_{90}Rh_{10}$ thermocouples, with no correction for the effect of pressure on emf. The combined accuracy and precision in reported temperature is estimated to be ± 5°C. Pressure was maintained to within 200 bar gauge pressure. Rapid quenching was achieved by cutting power to the apparatus, which cooled the experiments to approximately 50°C in approximately 1 min (Manning & Boettcher 1994; Manning 1994).

After each experiment, capsules were cleaned and then punctured to extract the quenched fluid. This was initially done directly by a micropipette, with subsequent dilution in nanopure H_2O; however, some solution occasionally sprayed from the puncture in some experiments. In such cases it could not be demonstrated that the extracted fluids were faithful samples of the quench fluid, and these runs were discarded. To avoid this problem, a Teflon extraction vessel was used (Manning & Boettcher 1994), which facilitated consistently accurate fluid sampling. Capsules were punctured in 15 ml of 5% HNO_3 and decanted after allowing >3 h for mixing of quench solute and diluent. Blank tests on kyanite crystals yielded no detectable Al or Si. Diluted experimental solutions were analyzed for Al and Si

concentrations by inductively coupled plasma (ICP) emission spectroscopy using carefully prepared Si and Al standard solutions. Six to nine counting periods were used during analysis. Unless otherwise noted, reported uncertainties are propagated 1σ analytical errors. Solid products were mounted on aluminum stubs for optical and scanning electron microscope (SEM) study of textures and phases.

RESULTS

Results are presented in Table 1. Reported concentrations are weighted means of multiple ICP analysis cycles; differences in concentration uncertainties reflect varying instrument conditions and standardization characteristics. Other potential sources of error include diluent volumes and mass of H_2O in experiments. Estimated errors in diluent volumes were <1%, which leads to errors smaller than analytical errors; they are therefore ignored. Errors in H_2O in the experimental charge arise from water loss during welding. If the typical 0.1 mg welding-related weight loss was H_2O, solubilities in Table 1 would require upward adjustment of Al and Si molality (m_{Al} and m_{Si}) of less than approximately 10^{-5} and approximately 10^{-3}, respectively. Because these errors are small compared to analytical uncertainty, they were ignored with one exception. A large, non-negligible welding weight loss of 5.56 mg occurred during preparation of Experiment 402 (Table 1), and concentrations are reported as the midpoint between the maximum and minimum values that result from incorporating this uncertainty.

Kyanite + H_2O starting materials

Initial experiments were designed to determine fluid compositions in equilibrium with kyanite + corundum by dissolving kyanite in pure H_2O. The greater solubility of Si relative to Al caused nucleation and growth of hexagonal corundum platelets on kyanite surfaces (Fig. 1). Nine replicate experiments at 700°C and 10 kbar yielded substantial growth of corundum on kyanite surfaces (Fig. 1). However, as shown in Table 1 and Fig. 2, Al and Si concentrations showed erratic variations independent of run duration ($m_{Al} = 0.002–0.023$ and $m_{Si} = 0.076–0.425$). Only pure H_2O was used, so equilibrium pH differences between experiments are implausible. The erratic Al concentrations show no correlation with experiment duration, mass of kyanite, or fluid volume (Table 1). Moreover, there was no textural evidence for significant quench solids (Fig. 1).

Scanning electron microscope petrography revealed that kyanite surfaces were entirely coated by corundum in four of these experiments (Fig. 1A), but that the corundum sheath was incomplete in the other five (Fig. 1C). Fluid compositions correlate with these textural differences. Figure 2 shows that experiments producing partly coated kyanite gave inconsistent Al solubility. By contrast, when kyanite was completely covered by corundum, a narrow range of Al solubility was observed. Moreover, the Al solubility recorded when kyanite was partly coated was either higher or lower than, but not the same as, that in solutions coexisting with fully coated kyanite (Fig. 2).

These observations imply that partial coating records incomplete equilibration, such that resulting fluids were either supersaturated or undersaturated metastably with respect to corundum + kyanite, whereas full development of a corundum sheath reflects equilibrium conditions. Presumably, the initially strong undersaturation of the pure H_2O starting fluid led to an erratic approach to equilibrium. In some instances, persistent metastable fluid compositions and textures were produced, while in others, equilibrium was approached closely. Although it is commonly assumed

Table 1 Experimental results at 700°C, 10 kbar.

Expt. No.	Duration (h)	Starting materials	Start H_2O (ml)	Start SiO_2 (mg)	Start Al_2O_3 (mg)	Extraction method	Final Si (molal)	Final Al (mmolal)	Result
364	48	KW	63.26	–	–	MP	0.425 (09)	23.39 (09)	Partial co coat on ky
369	24	KW	55.24	–	–	MP	0.422 (04)	9.95 (06)	Partial co coat on ky
372	69	KW	59.04	–	–	EV	0.076 (01)	1.75 (01)	Partial co coat on ky
376	95	KW	55.08	–	–	EV	0.305 (02)	11.99 (01)	Partial co coat on ky
377	24	KW	71.46	–	–	EV	0.206 (01)	2.70 (26)	Partial co coat on ky
363	24	KW	72.02	–	–	MP	0.333 (01)	6.30 (33)	Complete co coat on ky
365	73	KW	54.89	–	–	MP	0.377 (04)	5.87 (06)	Complete co coat on ky
366	7.5	KW	67.48	–	–	MP	0.286 (02)	6.27 (40)	Complete co coat on ky
370	48	KW	60.37	–	–	MP	0.336 (02)	5.53 (10)	Complete co coat on ky
398	24	KCW	69.06	–	1.41	EV	0.147 (01)	2.01 (02)	Partial co coat on ky
400	47	KQW	60.30	0.89	–	EV	0.293 (01)	2.99 (01)	Partial co coat on ky
409	67	KQW	76.45	0.50	–	EV	0.281 (01)	5.73 (04)	Partial co coat on ky
402	89	KQAW	72.36	0.96	0.20	EV	0.292 (12)	6.64 (27)	Partial co coat on ky

Parenthetical numbers are weighted 1σ analytical uncertainties, except 402, for which errors indicate range between minimum and maximum due to welding weight loss of 5.56 mg. K, kyanite; W, H_2O; C, corundum chip (single crystal); Q, quartz powder; A, γ-Al_2O_3 powder; MP, micropipette; EV, extraction vessel (see text); co, corundum; ky, kyanite.

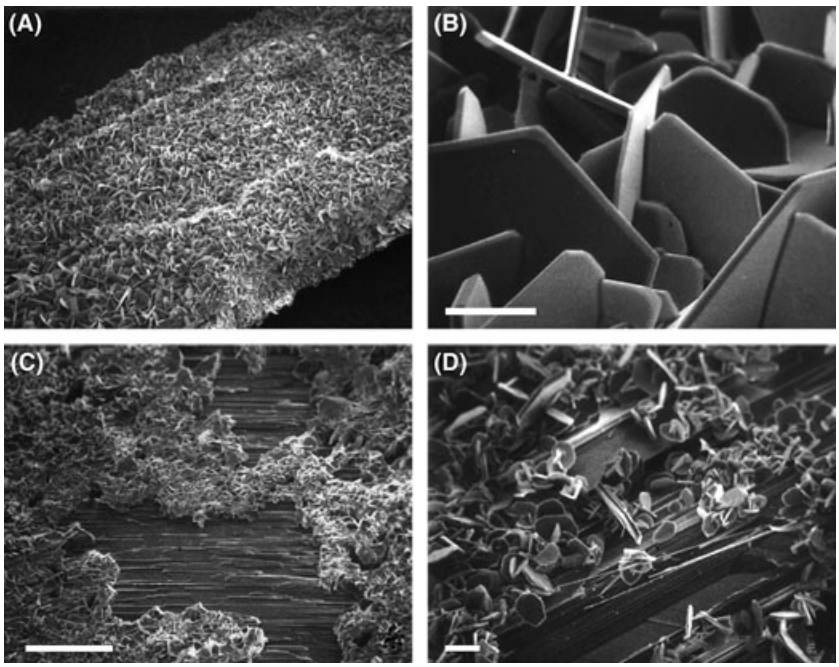

Fig. 1. Secondary electron photomicrographs of experimental run products. (A) Full corundum coating on kyanite crystal; crystal is approximately 2 mm across. (B) Interlocking, hexagonal corundum crystals; Run 369; scale bar is 15 μm. (C) Partial corundum coating with etched kyanite surface beneath; Run 366; scale bar is 100 μm. (D) Corundum crystals and etched kyanite surface in Run 400, with kyanite + quartz powder starting materials; scale bar is 15 μm.

that mineral layers prevent attainment of equilibrium, the corundum coatings were easily disaggregated or cut off, and examination in cross section revealed them to be loose, porous layers of randomly oriented corundum flakes (Fig. 1). Such loose layers are not likely to have impeded fluid access to the kyanite surfaces.

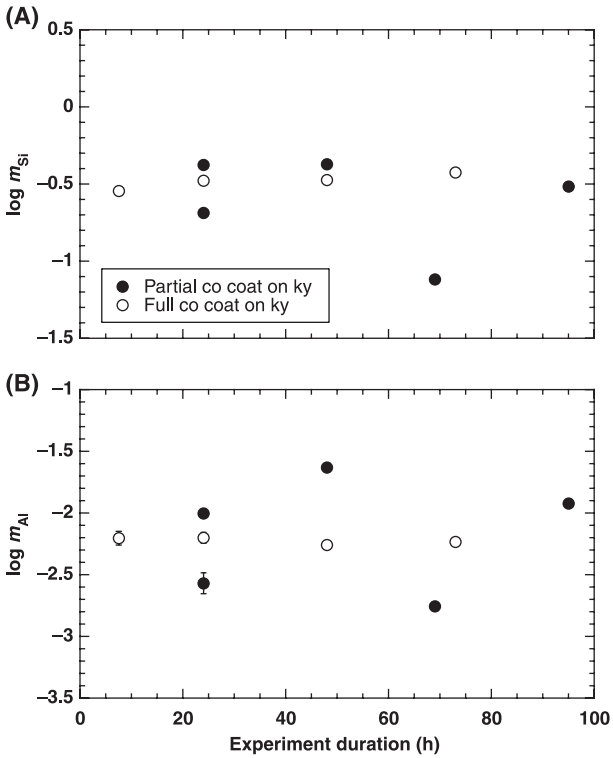

Fig. 2. Variation in Si (A) and Al (B) concentration (log molality) with duration in kyanite + H_2O experiments, 700°C, 10 kbar. Error bars show 2σ analytical uncertainty where larger than the symbol size. Experiments in which a full corundum (co) coat developed (open circles) on kyanite (ky) show more consistent final concentrations than those in which only a partial coat grew (filled circles).

Kyanite + H_2O + corundum chip starting materials

In an attempt to drive solutions to equilibrium more effectively, a single ultrapure synthetic corundum chip was included with kyanite and H_2O and held at 700°C, 10 kbar for 24 h (Run 398, Table 1). Irregular dissolution pits developed on the corundum crystal and an incomplete corundum layer grew on the kyanite. Measured aqueous Al and Si contents were 0.201 ± 0.003 mmol kg^{-1} and 0.146 ± 0.002 mol kg^{-1}, respectively. These concentrations are lower than all but one of the experiments in which only kyanite was placed in the charge. This result suggests that equilibration was also a problem in this experiment. If single crystals can be used to circumvent the inferred erratic approach to equilibrium, then run durations significantly longer than 24 h are likely required.

Kyanite + quartz-Al_2O_3 powders + H_2O starting materials

As an alternative test of the hypothesis that strong initial undersaturation led to erratic results, starting solutions closer to the predicted final composition were generated within the charge. The high solubilities at the experimental conditions prevented simple preparation of such fluids at 1 atm and 25°C. Instead, powdered natural quartz ± synthetic anhydrous γ-Al_2O_3 were added with the kyanite crystals. Because of the high surface area of the powders, their dissolution rate was likely much greater than that of

the larger kyanite crystals, which would have caused fluid composition to evolve rapidly to slightly supersaturated or undersaturated compositions prior to significant kyanite dissolution. Powder weights corresponded to a desired starting fluid composition near the predicted phase boundary, assuming complete dissolution. In addition to testing the idea that the extent of corundum coating is a guide to equilibration, these experiments also provide compositional reversals because the final composition could be approached from different directions.

Multiple experiments were conducted using varying amounts of powders (Table 1). Partial corundum coatings grew on kyanite surfaces in all these runs (Fig. 1D), as anticipated from the different quantities of SiO_2 and Al_2O_3 added. Note that the partial coating in this set of experiments is expected due to the smaller mass of kyanite that must be dissolved to attain equilibrium, rather than disequilibrium. As illustrated in Fig. 3, the Si and Al concentrations in the two longer runs of this type (>60 h) agree well with the concentrations in the kyanite + H_2O experiments in which a complete corundum coat was produced. Run 402 contained γ-Al_2O_3 powder in excess of predicted total dissolved Al; if all powder initially dissolved, this experiment would have approached equilibrium from supersaturation. Run 400 was shorter in duration (47 h) and contained no Al_2O_3 powder. This experiment yielded Si concentration similar to the other two, but lower Al (Fig. 3, Table 1).

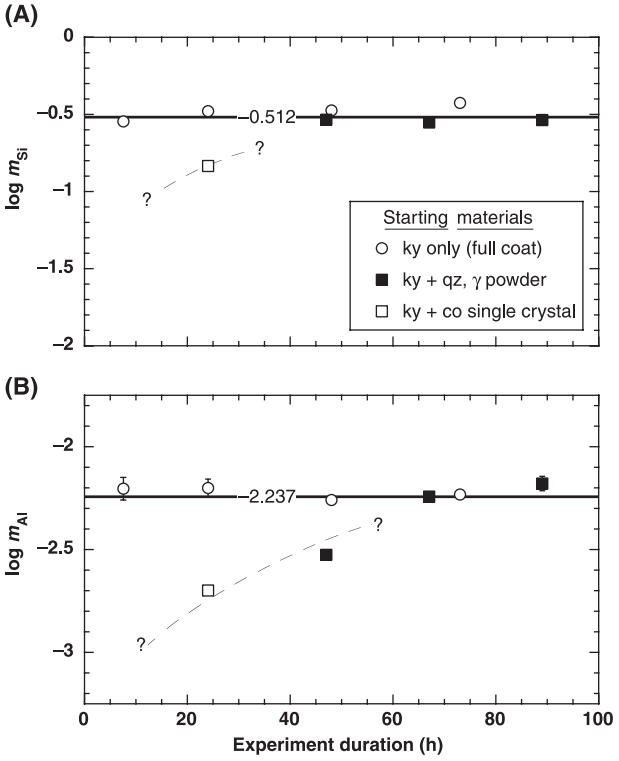

Fig. 3. Variation in Si (A) and Al (B) concentration (log molality) with duration for experiments with different starting materials, 700°C, 10 kbar: open circles, kyanite (ky) only runs in which full corundum coat grew; filled squares, kyanite + quartz (qz) and/or γ-Al_2O_3 (γ) powders; open square, kyanite and corundum (co) single crystal. Bold horizontal lines show inferred equilibrium Si and Al concentrations, as determined by weighted mean of experiments interpreted to reflect equilibrium (values given in log molality; see text). Queried dashed lines show postulated approach to equilibrium.

DISCUSSION

Equilibrium fluid compositions

Two sets of experiments are interpreted to constrain equilibrium Al and Si contents at 700°C, 10 kbar: kyanite-only experiments in which a complete corundum coating developed (runs 363, 365, 366, and 370), and kyanite-powder runs >60 h in duration in which corundum was saturated (runs 402 and 409). These six experiments yield weighted mean $m_{Al} = 5.80 \pm 0.03 \times 10^{-3}$ and $m_{Si} = 0.308 \pm 0.003$ mol kg^{-1} H_2O (Fig. 3). As noted above, runs 398 and 400 were omitted because run times were evidently too short, and the kyanite-only experiments with incomplete coats were rejected because they display textural evidence for partial equilibration which correlates with erratic final compositions. The more rapid, erratic approach to equilibrium in kyanite-only experiments is plausible because of greater initial disequilibrium between H_2O and kyanite relative to Si-Al-bearing H_2O and kyanite in the other configurations.

It is possible that the interpretation of disequilibrium in some experiments is incorrect. If all results are averaged, mean Al and Si molalities would be $7 \pm 6 \times 10^{-3}$ and 0.3 ± 0.1 molal. These values differ from the preferred results chiefly in their larger uncertainties.

Comparison to previous results

Corundum solubility in H_2O was measured at 700°C, 10 kbar by Becker *et al.* (1983) and Tropper & Manning (2007). Results of these two studies show that Al concentrations increase strongly with pressure. At 700°C, 10 kbar, the two studies are in good agreement, giving measured total Al concentration of 1.85 ± 0.13 mmolal (Becker *et al.* 1983) and 1.2 ± 0.2 mmolal (Tropper & Manning 2007). These Al concentrations are significantly lower than the value of 5.80 ± 0.03 mmolal measured in the present study. The greater Al concentration in Si-bearing solutions is a strong indication of Si-Al complexing.

Silicon concentrations in equilibrium with kyanite and corundum have not previously been measured at 700°C, 10 kbar; however, Newton & Manning (2003) found that, at 800°C and 12 kbar, Si molalities in equilibrium with quartz and kyanite + corundum were 1.413 and

0.984, respectively, giving a difference (Δm_{Si}) of 0.429 molal. At 700°C, 10 kbar, quartz solubility is 0.757 molal (Manning 1994), which, when combined with the Si content in equilibrium with kyanite + corundum determined in the present study (0.308 molal), gives a very similar Δm_{Si} of 0.449 molal. Because the small change in chemical potential difference over this *P*–*T* range should result in comparatively minor shifts Δm_{Si}, the similarity in these values lends confidence that equilibrium was approached in the present study.

Thermodynamic analysis

The larger solubility of corundum in Si-bearing fluids than in pure H_2O could be due either to pH effects or complexing with Si. However, enhancement of Al solubility by shifting pH to stabilize charged Al-hydroxide species [e.g., $Al(OH)_4^-$, $Al(OH)_2^+$, etc.] is unlikely because the only additional component in the solutions is Si. Rather, the increase in Al solubility more probably indicates the formation of Al-Si complexes in solution. As shown below, the thermodynamic properties of Al-Si complex(es) can be evaluated in light of data on aqueous Al hydroxides and Si species and the results of the present study.

Al hydroxide species in the system Al-O-H

Pokrovskii & Helgeson (1995) derived thermodynamic properties of aqueous Al hydroxide species based in part on the high *P* and *T* corundum solubility data of Becker *et al.* (1983). They found that at 700°C, 5 kbar, the only relevant species were $Al(OH)_3^\circ$ and $Al(OH)_4^-$ over a wide range of pH of approximately 1 to >8. Following Pokrovskii & Helgeson, these species are referred to below as $HAlO_{2,aq}$ and AlO_2^- for simplicity; by convention, the changes in standard molal Gibbs energy of reaction (ΔG_r°) for the equilibria $HAlO_{2,aq} + H_2O = Al(OH)_3^\circ$ and $AlO_2^- + 2H_2O = Al(OH)_4^-$ are zero.

Pokrovskii & Helgeson (1995) used the Helgeson–Kirkham–Flowers equation of state (Helgeson *et al.* 1981; Tanger & Helgeson 1988), which is considered accurate to a maximum pressure of 5 kbar. However, their data can be extrapolated to 10 kbar using the approach of Manning (1998). Equilibrium constants (*K*) for the equilibria

$$\underset{\text{corundum}}{Al_2O_3} + H_2O = 2HAlO_{2,aq} \quad (1)$$

and

$$HAlO_{2,aq} = H^+ + AlO_2^- \quad (2)$$

were calculated using data for aqueous Al species from Pokrovskii & Helgeson (1995) and for minerals from SUPCRT92 (Johnson *et al.* 1992). Properties of H_2O are from Haar *et al.* (1984), as calculated by SUPCRT92. In all calculations, standard states for minerals and H_2O were unit activity of the pure phase, and for aqueous species, unit activity of the hypothetical 1 molal solution referenced to infinite dilution. Activity coefficients of neutral complexes were assumed to be unity; concentrations of charged species were low ($<10^{-3}$ molal), and activity coefficients were therefore also assumed to be unity.

Values of $\log K_1$ and $\log K_2$ vary linearly with the logarithm of H_2O density at $P \geqslant 3$ kbar (Fig. 4). This linearity arises from the fact that $(\partial \ln K/\partial \rho_{H_2O})_T = -\Delta V_r^\circ/\beta_{H_2O}RT$ (where β is the coefficient of isothermal compressibility), and $\Delta V_r^\circ/\beta_{H_2O}$ approaches a constant value at high *P*. Because the product *RT* is also constant along isotherms, the dependence of $\log K$ on $\log \rho_{H_2O}$, depicted in Fig. 4, is expected to be linear at high H_2O density. Linear fits at 700°C and $\geqslant$3 kbar give

$$\log K_1 = 6.177 \log \rho_{H_2O} - 5.745 \quad (3)$$

and

$$\log K_2 = 6.633 \log \rho_{H_2O} - 4.730 \quad (4)$$

The uncertainty in the thermodynamic data is poorly known, but is estimated to be ± 500 cal mol^{-1} (e.g., Shock & Helgeson 1988). Figure 4 shows that linear extrapolations to high *P* using Eqns 3 and 4 are reasonable in light of these uncertainties. Calculated values of $\log K_1$ and $\log K_2$ at the experimental conditions are given in Table 2.

The extrapolation scheme outlined above can be tested by comparing corundum solubility in H_2O calculated from the derived equilibrium constants with experimental

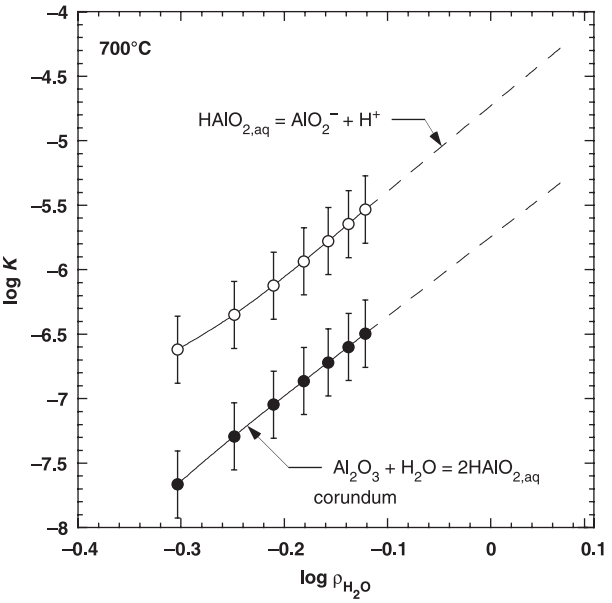

Fig. 4. Log ρ_{H_2O} versus log *K* at 700°C for reactions (1) and (2) (text). Circles show calculated values from 2 to 5 kbar at 0.5 kbar increments (SUPCRT92) with 500 cal mol^{-1} estimated uncertainty (Shock & Helgeson 1988). Dashed lines are extrapolations to 25 kbar based on linear fits to 3–5 kbar values (equations 3 and 4, text).

Table 2 Summary of thermodynamic data at 700°C, 10 kbar.

System	Phase, species, or equilibrium	Equation	ρ (g cm^{-3})	log K	ΔG° (kJ mol^{-1})*	Source
O-H	H_2O		0.944		−295.6	1
	$H_2O = H^+ + OH^-$	5		−7.580		2
Al-O-H	Corundum + $H_2O = 2HAlO_{2,aq}$	1		−5.900		4
	$HAlO_{2,aq} = H^+ + AlO_2^-$	2		−4.896		4
	Corundum				−1625.3	1
	$HAlO_{2,aq}$				−905.5	4
	AlO_2^-				−814.3	4
Si-O-H	Quartz				−887.8	1
	Quartz = $SiO_{2,aq}$	10		−0.543		3
	$2SiO_{2,aq} = Si_2O_{4,aq}$	8		0.452		3
	$SiO_{2,aq}$				−877.7	4
	$Si_2O_{4,aq}$				−1763.7	4
Al-Si-O-H	Kyanite				−2517.9	1
	Kyanite = corundum + $SiO_{2,aq}$	14		−0.800		4
	Kyanite + $H_2O = 2HAlO_{2,aq} + SiO_{2,aq}$	16		−6.700		4
	$HAlO_{2,aq} + SiO_{2,aq} = HAlSiO_{4,aq}$	12		1.414		4
	$HAlSiO_{4,aq}$				−1809.5	4

Data sources: 1, SUPCRT92 (Johnson *et al.* 1992); 2, Marshall & Franck (1981); 3, Manning (1994) and Newton & Manning (2002) (converted from mole fraction to molality scale); 4, This study.
*ΔG° indicates conventional apparent standard molal Gibbs energy (Benson–Helgeson) at 700°C, 10 kbar.

measurements. Corundum solubility was computed by combination of mass-action equations for equilibria 1, 2 and H_2O dissociation:

$$H_2O = H^+ + OH^- \tag{5}$$

(Table 2), along with the charge-balance constraint

$$m_{H^+} = m_{AlO_2^-} + m_{OH^-} \tag{6}$$

which leads to

$$m_{H^+} = (K_1^{1/2}K_2 + K_5)^{1/2} \tag{7}$$

Solution of Eqn 7 using data from Table 2 gives m_{H^+} and allows concentrations of remaining species to be calculated by back substitution. This gives $m_{HAlO_{2,aq}} = 1.12$ mmolal and $m_{AlO_2^-} = 0.07$ mmolal, or total Al concentration in H_2O in equilibrium with corundum of 1.19 mmolal, in excellent agreement with the 1.2 ± 0.2 mmolal value of Tropper & Manning (2007), but slightly lower than the result of Becker *et al.* (1983).

The results show that independently calculated solubility agrees well with experiments in H_2O at 10 kbar and 700°C. This supports the conclusion based on the present experimental results that the higher corundum solubility in Si-bearing fluids results from Al-Si interaction in the aqueous phase. However, evaluation of the thermodynamic properties of Al-Si species first requires determination of the properties of Si species in the Al-free Si-O-H system.

Silica species in the system Si-O-H

In SiO_2-H_2O fluids at high P and T, silica occurs primarily as monomers ($SiO_{2,aq}$, equivalent to H_4SiO_4) and dimers ($Si_2O_{4,aq}$, equivalent to $H_6Si_2O_7$) (Zhang & Frantz 2000; Zotov & Keppler 2000, 2002; Newton & Manning 2002, 2003). Newton & Manning (2002, 2003) showed that monomers and dimers mix ideally, which allows the equilibrium constant for the reaction

$$2SiO_{2,aq} = Si_2O_{4,aq} \tag{8}$$

to be written

$$K_8 = \frac{m_{Si_2O_{4,aq}}}{m^2_{SiO_{2,aq}}} \tag{9}$$

At 700°C and 10 kbar, Newton & Manning (2002) give $K_8 = 2.83$ (converted from mole fraction concentration scale). Using their equations for calculating species concentrations at quartz saturation yields $m_{SiO_{2,aq}} = 0.286$ and $m_{Si_2O_{4,aq}} = 0.232$. Equilibrium between quartz and silica monomers is described by

$$\underset{\text{quartz}}{SiO_2} = SiO_{2,aq} \tag{10}$$

which allows derivation of the standard molal Gibbs energy of monomeric $SiO_{2,aq}$ at 700°C, 10 kbar, from

$$\Delta G^\circ_{SiO_{2,aq}} = \Delta G^\circ_{qz} - RT\ln K_{10} = \Delta G^\circ_{qz} - RT\ln m_{SiO_{2,aq}} \tag{11}$$

Using ΔG°_{qz} from Table 2 gives $\Delta G^\circ_{SiO_{2,aq}}$ kJ mol^{-1}. A similar approach was used to derive $\Delta G^\circ_{Si_2O_{4,aq}}$ (Table 2).

Al-Si species in the system Al-Si-O-H

Combination of the data for Al hydroxide and silica species (Table 2) with experimental results of the present study permits derivation of the thermodynamic properties of Al-Si complexes. At low P and T, charged Al-Si species are

evidently more stable than neutral complexes and are abundant primarily in acidic or basic solutions (Pokrovski *et al.* 1996; Salvi *et al.* 1998); however, at high *P* and *T*, it is likely that, as with Al-hydroxide species, neutral species predominate over a wide range of pH. Because the present experiments did not control pH, or examine corundum + kyanite solubility as a function of pH, it is not possible to determine the charge or stoichiometry of the Al-Si solutes. Accordingly, it is assumed here that any Al-Si complexing occurs by formation of the neutral complex $HAlSiO_{4,aq}$. Although it is likely that the neutral species predominates, the thermodynamic properties derived for this species necessarily reflect only the sum of all Al-Si complexes present in the experimental solutions.

Thermodynamic properties of $HAlSiO_{4,aq}$ can be derived from the present experiments by writing the homogeneous equilibrium

$$HAlO_{2,aq} + SiO_{2,aq} = HAlSiO_{4,aq} \quad (12)$$

for which

$$K_{12} = \frac{a_{HAlSiO_{4,aq}}}{a_{HAlO_{2,aq}} a_{SiO_{2,aq}}} \quad (13)$$

Activities in the right-hand quotient can be determined from the thermodynamic data in Table 2, results of the corundum-kyanite experiments, and the assumption that $a_i = m_i$ for neutral species. This gives $a_{HAlO_{2,aq}} = 1.12$ at corundum saturation. The activity of $SiO_{2,aq}$ monomers can be derived from the equilibrium

$$\underset{\text{kyanite}}{Al_2SiO_5} = \underset{\text{corundum}}{Al_2O_3} + SiO_{2,aq} \quad (14)$$

for which $K_{14}=a_{SiO_{2,aq}}=0.158$ from data in Table 2. Finally, $a_{HAlSiO_{4,aq}}$ can be calculated by mass balance

$$a_{HAlSiO_{4,aq}} = m_{HAlSiO_{4,aq}} = m_{Al,total} - m_{HAlO_{2,aq}} - m_{AlO_2^-} \quad (15)$$

to give $a_{HAlSiO_{4,aq}} = 0.00461$, $K_{12} = 25.91$ and $\Delta G^\circ_{HAlSiO_{4,aq}} = -1809.5$ kJ mol^{-1} (Table 2).

Speciation of Al-Si-O-H fluids

The thermodynamic data derived above provide a basis for predicting the influence of silica on aqueous Al concentrations derived by dissolution of corundum and kyanite. For example, the equilibrium constant for the kyanite dissolution reaction

$$\underset{\text{kyanite}}{Al_2SiO_5} + H_2O = 2HAlO_{2,aq} + SiO_{2,aq} \quad (16)$$

is

$$K_{16} = a^2_{HAlO_{2,aq}} a_{SiO_{2,aq}} \quad (17)$$

at unit activities of kyanite and H_2O. The value of log K_{16} is −6.700 (Table 2), as derived from $a_{HAlO_{2,aq}}$ and $a_{SiO_{2,aq}}$ at kyanite-corundum equilibrium. In the absence of Al-Si complexing, increasing $m_{Si,total}$ will lead to increasing activity of monomeric $SiO_{2,aq}$, which in turn would require that $m_{HAlO_{2,aq}}$ decrease as its square; that is, if the only significant Al species is $HAlO_{2,aq}$, then with increasing $m_{Si,total}$, $m_{Al,total}$ should decline from a maximum at corundum saturation until quartz saturation is attained (Fig. 5A). However, interaction of Al and Si to form complexes, here modeled as $HAlSiO_{4,aq}$, is strongly favored energetically, by virtue of the relatively large value of K_{12} of 25.91 derived from the present experiments. Thus, in silica-bearing solutions, Al-Si interaction will remove $HAlO_{2,aq}$ and $SiO_{2,aq}$ (Eqn 12), driving the kyanite dissolution reaction (Eqn 16) to the right. The result is that, at equilibrium, $m_{Al,total}$ is higher than predicted assuming simple Si-free Al hydroxide species and reaches a maximum at quartz saturation.

These observations can be quantified by computing the changes in species abundances with $m_{Si,total}$. By specifying the concentration of $SiO_{2,aq}$ monomers and using the thermodynamic data in Table 2, the following equations constrain the concentrations of the other aqueous species:

$$m_{SiO_{4,aq}} = K_8 m^2_{SiO_{2,aq}}$$
$$m_{HAlO_{2,aq}} = K_1^{1/2} \text{(corundum stability field)}$$
$$m_{HAlO_{2,aq}} = (K_{16}/m_{SiO_{2,aq}})^{1/2} \text{(kyanite stability field)}$$
$$m_{HAlSiO_{4,aq}} = K_{14} m_{HAlO_{2,aq}} m_{SiO_{2,aq}}$$
$$m_{H^+} = (K_2 K_1^{1/2} + K_5)^{1/2}$$
$$m_{OH^-} = K_5/m_{H^+}$$
$$m_{AlO_2^-} = K_2 m_{HAlO_2}/m_{H^+}$$
$$m_{Si,total} = m_{SiO_{2,aq}} + 2m_{Si_2O_{4,aq}} + m_{HAlSiO_{4,aq}}$$
$$m_{Al,total} = m_{HAlO_{2,aq}} + m_{AlO_2^-} + m_{HAlSiO_{4,aq}}$$

Unit activity coefficients were assumed in all calculations.

The results of the speciation calculation in the system Al-Si-O-H are shown in Fig. 5B. The speciation depends on the mineral with which the fluid coexists. With increasing $m_{Si,total}$ in the corundum stability field, $m_{HAlO_{2,aq}}$, $m_{AlO_2^-}$, m_{OH^-} and pH are constant, but $m_{Al,total}$ increases due to increasing $m_{HAlSiO_{4,aq}}$. The low but non-negligible AlO_2^- molality shifts calculated pH from neutrality (pH = 3.79) to the slightly acidic value of 3.70. In the kyanite stability field, the dependence of $m_{HAlSiO_{4,aq}}$ and $m_{Al,total}$ on Si change because of the decrease in $m_{HAlO_{2,aq}}$ and $m_{AlO_2^-}$; nevertheless, $m_{Al,total}$ continues to increase until it reaches a maximum at quartz saturation. The decrease in $m_{AlO_2^-}$ also produces a slight increase in pH to 3.72 at kyanite-quartz equilibrium. Silica speciation is a strong function of total dissolved silica; at corundum-kyanite equilibrium, Si is partitioned subequally between monomers (53%) and dimers (47%) on a molar basis. Calculated

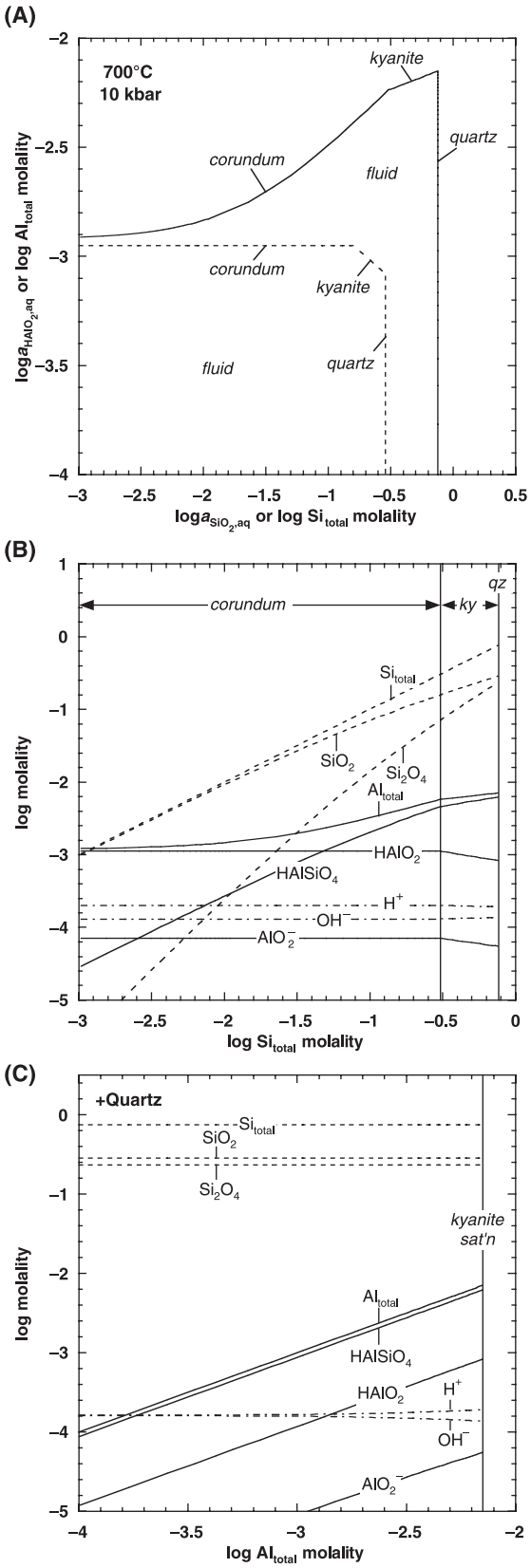

Fig. 5. (A) Comparison of variations in activities of Al and Si neutral monomers ($HAlO_{2,aq}$ and $SiO_{2,aq}$; dashed lines) with total Al and Si molalities (solid lines) at corundum, kyanite and quartz saturation, 700°C, 10 kbar. The difference between the dashed and solid lines illustrates the consequences of Al-Si interaction and Si polymerization, and shows that the maximum Al concentrations in the system Al-Si-O-H are predicted to occur at kyanite + quartz equilibrium. (B) Equilibrium abundances of aqueous species coexisting with corundum or kyanite as a function of total Si molality at 700°C, 10 kbar. Dashed lines, major Si species; solid lines, major Al species; dash-dot lines, H^+ and OH^-. (C) Equilibrium abundances of aqueous species coexisting with quartz as a function of total Al molality at 700°C, 10 kbar. Lines as in (B).

$m_{Si,total}$ at kyanite-corundum equilibrium is 0.305 molal, in excellent agreement with the measured Si concentration of 0.308 ± 0.003 molal.

A similar approach can be used to predict speciation at quartz saturation as a function of $m_{Al,total}$ (Fig. 5C). At these conditions, $SiO_{2,aq}$ and $Si_2O_{4,aq}$ are constant, but $m_{Al,total}$ and $m_{HAlSiO_{4,aq}}$ increase sympathetically. The increase in $m_{HAlSiO_{4,aq}}$ contributes to a slight rise in total dissolved silica that is not resolvable on the scale of Fig. 5C. A small pH decrease with $m_{Al,total}$ arises from the increase in m_{Al}.

Implications for Al transport during high-P metamorphism

The formation of Al-Si complexes leads to a substantial increase in Al solubility beyond that predicted if only aluminum hydroxides are considered (Fig. 5A). Figure 5B,C illustrates that Al-Si complexes will host most of the Al in Si-bearing H_2O at 700°C, 10 kbar, which results from the large value of K_{12} constrained by the experiments. The molality of $HAlSiO_{4,aq}$ is greater than that of $HAlO_{2,aq}$ for all $m_{Si,total} \geq 0.05$. The $m_{Si,total}$ of the equivalence point is well below that of a fluid in equilibrium with a model upper mantle mineral assemblage, including forsterite and enstatite ($m_{Si,total}$ approximately 0.14), suggesting that Al-Si complexes will be the predominant form of dissolved Al in all lower crustal, mantle, and subduction environments, in the absence of other complexing agents.

Although the experiments were conducted at a single P and T, they nevertheless can give some general insight into Al mobility in high-P metasomatic environments. For example, the prediction that Al solubility is greatest at kyanite-quartz equilibrium in the system Al-Si-O-H helps explain the common observation of kyanite + quartz segregations in high-P metamorphic rocks, such as eclogites. Based on the present findings, these features may result from the high Al solubility in Si-bearing fluids, which permits growth of kyanite + quartz from lower fluid volumes than if Si were not present. Extending the results still further, the formation of polymeric speices is favored by increasing pressure in the system Si-O-H (Newton &

Manning 2002; Zotov & Keppler 2002; Gerya *et al.* 2005). If this is also true when Al is added, then it is likely that Al enhancement by Si becomes less pronounced at lower pressures. This would lead to a larger isothermal dependence of Al solubility on pressure when Si is present than in the Al-O-H system. Thus, andalusite-quartz or sillimanite-quartz segregations at low to moderate pressure may owe their origin to the large decreases in solubility that would attend fluid decompression during exhumation. More fundamentally, the apparent discrepancies between those metamorphic environments which display evidence for Al mobility and those that do not may simply reflect relatively minor differences in the magnitutde of fluid–rock interaction.

Al-Si species stoichiometry and future work

As discussed above, the experiments at a single *P*, *T*, pH, and $m_{Si,total}$ cannot constrain the stoichiometry or charge of the Al-Si complex or complexes. Additional experiments at a range of buffered pH values are clearly required to explore the charge of Al-Si complexes. Moreover, the increase in $m_{Al,total}$ with $m_{si,total}$ will differ with the average stoichiometric Al/Si ratio of the complexes. The calculations described above can be repeated by assuming different Al:Si ratios. Figure 6 shows that for arbitrary Al:Si ratios of 1:2, 1:1, and 2:1, the Al content of kyanite + quartz-saturated H_2O may be significantly greater or less than predicted for Al/Si = 1. But the figure also shows that the increase in $m_{Al,total}$ with Si content will have different slopes and curvatures.

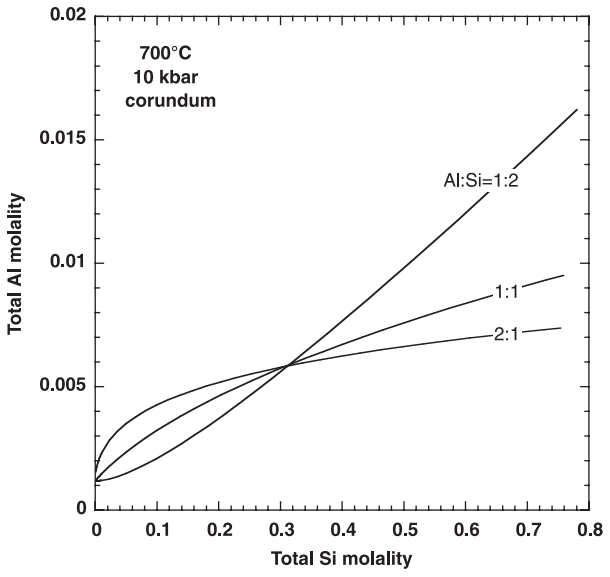

Fig. 6. Predicted variation in corundum solubility at 700°C, 10 kbar, as a function of total Si molality, assuming neutral Al-Si complexes with Si:Al ratios of 0.5, 1, and 2. The curves are constrained to be equal at corundum solubility in pure H_2O and at corundum-kyanite equilibrium. The contrasting slopes and curvatures indicate that experimental measurement of corundum solubility at very low Si content, and metastably at high Si content in the kyanite field ($m_{Si,total}$ > 0.31) will allow robust detection of the average stoichiometry of Al-Si species in solution.

Future experimental study of corundum solubility as a function of Si content can provide the data to establish the dependence of corundum solubility on dissolved Si to rigorously determine the average stoichiometry of Al-Si complexes. It is important to note, however, that the solution may contain Al-Si complexes of different stoichiometries, and the average Al/Si ratio may itself vary with total dissolved silica. Nevertheless, the approach developed here can be used with such measurements to determine the average ratio as a function aqueous Si content.

ACKNOWLEDGEMENTS

This work was supported by NSF EAR-0337170. I thank S. Boettcher for assistance with the experiments, and S. Wong for help with SEM petrography. The manuscript was improved by critical comments by R. Newton and W. Dollase, and reviewers S. Wood and B. Yardley.

REFERENCES

Ague JJ (1994) Mass transfer during Barrovian metamorphism of pelites, south-central Connecticut. II: channelized fluid flow and the growth of staurolite and kyanite. *American Journal of Science*, **294**, 1061–134.

Ague JJ (1995) Deep-crustal growth of quartz, kyanite and garnet into large-aperture, fluid-filled fractures, north-eastern Connecticut, USA. *Journal of Metamorphic Geology*, **13**, 299–314.

Anderson GM, Burnham CW (1967) Reactions of quartz and corundum with aqueous chloride and hydroxide solutions at high temperatures and pressures. *American Journal of Science*, **265**, 12–27.

Anderson GM, Burnham CW (1983) Feldspar solubility and the transport of aluminum under metamorphic conditions. *American Journal of Science*, **283-A**, 283–97.

Azaroual M, Pascal ML, Roux J (1996) Corundum solubility and aluminum speciation in KOH aqueous solutions at 400°C from 0.5 to 2.0 kbar. *Geochimica et Cosmochimica Acta*, **60**, 4601–14.

Becker KH, Cemic L, Langer KEO (1983) Solubility of corundum in supercritical water. *Geochimica et Cosmochimica Acta*, **47**, 1573–8.

Bohlen SR, Montana A, Kerrick DM (1991) Precise determination of the equilibria kyanite = sillimanite and kyanite = andalusite and a revised triple point for Al_2SiO_5 polymorphs. *The American Mineralogist*, **76**, 677–80.

Burnham CW, Ryzhenko BN, Schitel D (1973) Water solubility of corundum at 500–800°C and 6 kbar. *Geochemistry International*, **10**, 1374.

Carmichael DM (1969) On the mechanism of prograde metamorphic reactions in quartz-bearing pelitic rocks. *Contributions to Mineralogy and Petrology*, **20**, 244–67.

Cesare B (1994) Synmetamorphic veining: origin of andalusite-bearing veins in the Vedrette di Ries contact aureole, eastern Alps, Italy. *Journal of Metamorphic Geology*, **12**, 643–53.

Diakonov I, Pokrovski G, Schott J, Castet S, Gout R (1996) An experimental and computational study of sodium-aluminum complexing in crustal fluids. *Geochimica et Cosmochimica Acta*, **60**, 197–211.

Gerya TV, Maresch WV, Burchard M, Zakhartchouk V, Doltsinis NL & Fockenberg T (2005) Thermodynamic modeling of solubility and speciation of silica in H_2O-SiO_2 fluid up to 1300°C and 20 kbar based on the chain reaction formalism. *European Journal of Mineralogy*, **17**, 269–83.

Grant JA (1986) The isocon diagram – a simple solution to Gresens' equation for metasomatic alteration. *Economic Geology*, **81**, 1976–82.

Gresens RL (1967) Composition-volume relationships of metasomatism. *Chemical Geology*, **2**, 47–65.

Gresens RL (1971) Application of hydrolysis equilibria to the genesis of pegmatite and kyanite deposits in northern New Mexico. *Mountain Geologist*, **8**, 3–16.

Haar L, Gallagher JS, Kell GS (1984) *NBS/NRC Steam Tables*. Hemisphere, New York, 320 pp.

Helgeson HC, Kirkham DH, Flowers GC (1981) Theoretical prediction of the thermodynamic behavior of aqueous electrolytes at high pressures and temperatures: IV. Calculation of activity coefficients, osmotic coefficients, and apparent molal and standard and relative partial molal properties to 600°C and 5 kb. *American Journal of Science*, **281**, 1249–1516.

Irving JD (1911) Some features of replacement ore-bodies, etc. *Journal of the Canadian Mining Institute*, **14**, 395–471.

Johnson JW, Oelkers EH, Helgeson HC (1992) SUPCRT92: a software package for calculating the standard molal thermodynamic perperties of minerals, gases, aqueous species, and reactions from 1 to 5000 bar and 0 to 1000°C. *Computers and Geosciences*, **18**, 899–947.

Kerrick DM (1988) Al_2SiO_5-bearing segregations in the Leopontine Alps, Switzerland: aluminum mobility in metapelites. *Geology*, **16**, 636–40.

Kerrick DM (1990) The Al_2SiO_5 polymorphs. *Reviews in Mineralogy*, **22**, 406.

Korzhinskiy MA (1987) The solubility of corundum in an HCl fluid and forms taken by Al. *Geochemistry International*, **24**, 105–10.

Lindgren W (1912) The nature of replacement. *Economic Geology*, **7**, 521–35.

Lindgren W (1918) Volume changes in metamorphism. *Journal of Geology*, **26**, 542–54.

Manning CE (1994) The solubility of quartz in H_2O in the lower crust and upper mantle. *Geochimica et Cosmochimica Acta*, **58**, 4831–9.

Manning CE (1998) Fluid composition at the blueschist-eclogite transition in the model system Na_2O-MgO-Al_2O_3-SiO_2-H_2O-HCl. *Schweizerische Mineralogische und Petrographische Mitteilungen*, **78**, 225–242.

Manning CE, Boettcher SL (1994) Rapid-quench hydrothermal experiments at mantle pressures and temperatures. *The American Mineralogist*, **79**, 1153–8.

Marshall WL, Franck EU (1981) Ion product of water substance, 0–1000°C, 1–10,000 bars: new international formulation and its background. *Journal of Physical and Chemical Reference Data*, **10**, 295–304.

McLelland J, Morrison J, Selleck B, Cunningham B, Olson C, Schmidt K (2002) Hydrothermal alteration of late- to post-tectonic Lyon Mountain granitic gneiss, Adirondack Mountains, New York: origin of quartz-sillimanite segregations, quartz-albite lithologies, and associated Kiruna-type low-Ti Fe-oxide deposits. *Journal of Metamorphic Geology*, **20**, 175–90.

Morey GW (1957) The solubility of solids in gases. *Economic Geology*, **52**, 225–51.

Nabelek PI (1997) Quartz-sillimanite leucosomes in high-grade schists, Black Hills, South Dakota: a perspective on the mobility of Al in high-grade metamorphic rocks. *Geology*, **25**, 995–8.

Newton RC, Manning CE (2002) Solubility of enstatite + forsterite in H_2O at deep crust/upper mantle conditions: 4 to 15 kbar and 700 to 900°C. *Geochimica et Cosmochimica Acta*, **66**, 4165–76.

Newton RC, Manning CE (2003) Activity coefficient and polymerization of aqueous silica at 800°C, 12 kbar, from solubility measurements on SiO_2-buffered mineral assemblages. *Contributions to Mineralogy and Petrology*, **146**, 135–43.

Newton RC, Manning CE (2006) Solubilities of corundum, wollastonite and quartz in H_2O-NaCl solutions at 800°C and 10 kbar: interaction of simple minerals with brines at high pressure and temperature. *Geochimica et Cosmochimica Acta*, **70**, 5571–82.

Oelkers EH, Helgeson HC (1988) Calculation of the thermodynamic and transport properties of aqueous species at high pressures and temperatures: Aqueous tracer diffusion coefficients of ions to 1000°C and 5 kb. *Geochimica et Cosmochimica Acta*, **52**, 63–85.

Pascal ML, Anderson GM (1989) Speciation of Al, Si, and K in supercritical solutions: experimental study and interpretation. *Geochimica et Cosmochimica Acta*, **53**, 1843–55.

Pokrovskii VA, Helgeson HC (1995) Thermodynamic properties of aqueous species and the solubilities of minerals at high pressures and temperatures: the system Al_2O_3-H_2O-NaCl. *American Journal of Science*, **295**, 1255–342.

Pokrovskii VA, Helgeson HC (1997) Thermodynamic properties of aqueous species and the solubilities of minerals at high pressures and temperatures: the system Al_2O_3-H_2O-KOH. *Chemical Geology*, **137**, 221–42.

Pokrovski GS, Schott J, Harrichoury JC, Sergeyev AS (1996) The stability of aluminum silicate complexes in acidic solutions from 25–150°C. *Geochimica et Cosmochimica Acta*, **60**, 2495–501.

Poldervaart A (1953) Petrological calculations in metasomatic processes. *American Journal of Science*, **251**, 481–504.

Ragnarsdóttir KV, Walther JV (1985) Experimental determination of corundum solubilities in pure water between 400–700°C and 1–3 kbar. *Geochimica et Cosmochimica Acta*, **49**, 2109–15.

Ridge JD (1949) Gain and loss of material in a series of replacements. *Geological Society of America Special Paper*, **68**, 252–3.

Salvi S, Pokrovski GS, Shott J (1998) Experimental investigation of aluminum-silica aqueous complexing at 300°C. *Chemical Geology*, **151**, 51–67.

Sanjuan B, Michard G (1987) Aluminum hydroxide solubility in aqueous solutions containing fluoride ions at 50°C. *Geochimica et Cosmochimica Acta*, **51**, 1823–31.

Sepahi AA, Whitney DL, Baharifar AA (2004) Petrogenesis of andalusite-kyanite-sillimanite veins and host rocks, Sanandaj-Sirjan metamorphic belt, Hamadan, Iran. *Journal of Metamorphic Geology*, **22**, 119–34.

Shock EL, Helgeson HC (1988) Calculation of the thermodynamic and transport properties of aqueous species at high pressures and temperatures: correlation algorithms for ionic species and equation of state predictions to 5 kb and 1000°C. *Geochimica et Cosmochimica Acta*, **52**, 2009–36.

Tagirov B, Schott J (2001) Aluminum speciation in crustal fluids revisited. *Geochimica et Cosmochimica Acta*, **65**, 3965–92.

Tanger JC, Helgeson HC (1988) Calculation of the thermodynamic and transport-properties of aqueous species at high-pressures and temperatures – revised equations of state for the

standard partial molal properties of ions and electrolytes. *American Journal of Science*, **288**, 19–98.

Tropper P, Manning CE (2007) The solubility of corundum in H_2O at high pressure and temperature and its implications for Al mobility in the deep crust and upper mantle. *Chemical Geology*, in press. doi: 1016/j.chemgeo.2007.01.012.

Verlaguet A, Brunet F, Goffé B, Murphy WM (2006) Experimental study and modeling of fluid reaction paths in the quartz-kyanite ± muscovite-water system at 0.7 GPa in the 350–550°C range: implications for Al selective transfer during metamorphism. *Geochimica et Cosmochimica Acta*, **70**, 1772–88.

Vernon RH (1979) Formation of late sillimanite by hydrogen metasomatism (base-leaching) in some high-grade gneisses. *Lithos*, **12**, 143–52.

Vidal O, Durin L (1999) Aluminum mass transfer and diffusion in water at 400–550°C, 2 kbar in the K_2O-Al_2O_3-SiO_2-H_2O system driven by a thermal gradient or by a variation of temperature with time. *Mineralogical Magazine*, **63**, 633–47.

Walther JV (1997) Experimental determination and interpretation of the solubility of corundum in H_2O between 350 and 600°C from 0.5 to 2.2 kbar. *Geochimica et Cosmochimica Acta*, **61**, 4955–64.

Walther JV (2001) Experimental determination and analysis of the solubility of corundum in 0.1 and 0.5 m NaCl solutions between 400 and 600°C. *Geochimica et Cosmochimica Acta*, **65**, 2843–51.

Whitney DL, Dilek Y (2000) Andalusite-sillimanite-quartz veins as indicators of low-pressure-high-temperature deformation during late-stage unroofing of a metamorphic core complex, Turkey. *Journal of Metamorphic Geology*, **18**, 59–66.

Widmer T, Thompson AB (2001) Local origin of high pressure vein material in eclogite facies rocks of the Zermatt-Saas zone, Switzerland. *American Journal of Science*, **301**, 627–56.

Yardley BWD (1977) The nature and significance of the mechanism of sillimanite growth in the Connemara Schists, Ireland. *Contributions to Mineralogy and Petrology*, **65**, 53–58.

Zaraisky GP (1994) The influence of acidic fluoride and chloride solutions on the geochemical behaviour of Al, Si and W. In: *Fluids in the Crust: Equilibrium and Transport Properties* (eds Shmulovich KI, Yardley BWD, Gonchar GG), pp. 139–61. Chapman & Hall, London, UK.

Zhang YG, Frantz JD (2000) Enstatite-forsterite-water equilibria at elevated temperatures and pressures. *The American Mineralogist*, **85**, 918–25.

Zotov N, Keppler H (2000) In-situ Raman spectra of dissolved silica species in aqueous fluids to 900°C and 14 kbar. *The American Mineralogist*, **85**, 600–4.

Zotov N, Keppler H (2002) Silica speciation in aqueous fluids at high pressures and high temperatures. *Chemical Geology*, **184**, 71–82.